Microvascular characteristics of human gliomas: comparative assessment with conventional and alternative analysis methods for DCE-MRI

J. U. Harrer[1], D. L. Buckley[2], H. A. Haroon[2], K. Embleton[2], C. Roberts[2], D. Balériaux[3], A. Jackson[2], G. J. Parker[2]

[1]Dept. of Neurology, Aachen University Hospital, Aachen, Germany, [2]Imaging Science and Biomedical Engineering, University of Manchester, Manchester, United Kingdom, [3]Service de Radiologie, Hopital Erasme, Clinique Universitaires de Bruxelles, Bruxelles, Belgium

Introduction Several microvascular parameters may be estimated with the use of kinetic models, such as the volume transfer constant (K^{trans}) between blood plasma and the extravascular extracellular space (EES) and the fractional volume of the plasma (v_p). This allows assessment of angiogenic activity in tumours and inflammatory processes [1-2]. These parameters can be derived from contrast agent (CA) concentration curves obtained from T_1-weighted dynamic contrast-enhanced (DCE) MRI by application of a kinetic model of CA distribution. The most commonly applied model is that of Tofts and Kermode (TK) [2], which is attractive due to its relative ease of application. The two main sources of error in the results obtained when using this model are the application of a standardized, assumed vascular input function that ignores the first pass of the CA bolus and misses out interindividual physiologic differences and secondly the assumption that the observed CA concentration change in each voxel solely reflects CA leakage into the EES. This leads to erroneously high K^{trans} values, caused by intravascular CA, which itself contributes to the signal increase often affecting many voxels. This effect has been named 'pseudopermeability' [4]. Alternative models have been designed to clearly separate extra- and intravascular contribution to signal enhancement incorporating individually measured AIF and v_p [5-8]. We aimed to compare the conventional kinetic model with two alternative models to assess their accuracy in analysing K^{trans} and v_p in high-grade gliomas, a highly vascular tumour type.

Methods Eighteen patients with histologically and/or clinically confirmed gliomas were included into this study (WHO °III: 3; WHO °IV: 15). Imaging was performed on 1.5 Tesla ACS Gyroscan NT-PT 6000 (Philips Medical Systems, Best, The Netherlands) machines at two sites using birdcage receive-only head-coils. Routine T_1- and T_2-weighted imaging preceded the dynamic studies. Sequence parameters of DCE studies: precontrast data set: 3 consecutive 3D RF-spoiled T_1-FFE acquisitions (flip angles: 2°/10°/35°). Dynamic imaging series: flip angle: 35°; TR/TE (ms): 4.2 /1.2; FOV: 250 mm; effective slice thickness: 3 mm (Fourier interpolation); slices: 25; matrix: 128 X 128; series of images obtained: 60; temporal resolution: approximately 6 s. The CA (0.1 mmol/kg of Gd-DTPA-BMA, Nycomed, Oslo, Norway) was administered manually as an i.v. bolus over approximately 4 s after the seventh dynamic scan followed by a flush of an equal amount of normal saline. In addition to the established TK model, two models applying individually measured AIF and incorporating v_p were used for analysis: a modification of the TK model (mTK) using the middle cerebral artery to derive an individual, unfitted AIF [6] and the first-pass model (FP), using the superior sagittal sinus for measurement of the vascular input function, which was then fitted to a gamma-variate [8]. Both methods explicitly aim to differentiate between signal enhancement due to CA leakage into the EES and intravascular contrast agent by additionally modelling v_p. Regions of interest (ROI) were drawn manually around the whole tumour on at least three consecutive slices of the dynamic series through the middle of the tumour volume. The non-enhancing part of the tumour was subtracted automatically by definition of 'true enhancement' as one standard deviation above the enhancement of normal brain. All three kinetic models were applied to estimate K^{trans} and where possible v_p from the ROIs; parametric maps were calculated from the entire slices. Friedman's test and Wilcoxon's signed rank test were applied to compare, and Spearman's correlation test to correlate values of K^{trans} and v_p of the three models. Scatter plots were produced to enable patient individual pixel-by-pixel analysis of K^{trans} and v_p of the different models from ROIs of single slices.

Results Figure 1 (a)-(c) shows parameter maps of K^{trans} obtained with the three models. The tumour is located in the right occipital region and high K^{trans} is typically detected in the tumour rim. As shown in a), K_{TK} parameter maps suffer from 'pseudopermeability' effects displaying numerous vessels. These were not visualized on K_{mTK} maps (b) and K_{FP}-maps (c) but appeared on the corresponding v_p-maps, indicating the failure of the TK model in commonly occurring vascular regions. K_{mTK} maps and K_{FP}-maps both accurately display the highly permeable choroid plexus and do not show evidence of vessels, implying that the introduction of the vascular term reduces the 'pseudopermeability' effect. Comparison of median K^{trans} values obtained from the three models showed no correlation between either K_{FP} and K_{TK} or K_{mTK} and K_{TK}. Values of K_{TK} were considerably higher than K_{mTK} and K_{FP} ($p<0.001$) and ranged from 0.113 to 1.338 min^{-1}, which is most likely being caused by the lack of an individualised vascular input function and again, pseudopermeability effects. K_{mTK} and K_{FP} were more comparable and were closely correlated ($\rho=0.744$), with K_{mTK} generally higher than K_{FP} ($p<0.001$). K_{mTK} yielded values from 0.028 to 0.142 min^{-1}, K_{FP} estimates ranged from 0.007 to 0.094 min^{-1}. Estimates of $v_{p(mTK)}$ and $v_{p(FP)}$ also showed a significant difference ($p<0.001$) but were very closely correlated ($\rho=0.901$). Figure 2 (a)-(b) displays scatter plots of a pixel-by-pixel analysis of K_{mTK} and K_{FP} (a) and $v_{p(mTK)}$ and $v_{p(FP)}$ (b) showing the close individual correlation of both estimates.

Conclusion The Tofts and Kermode model gave K_{TK} values that were spuriously high and the corresponding K_{TK} maps clearly demonstrated numerous vessels [4-5]. These results clearly emphasize the impact of the *individual* vascular input function and the importance of acquiring these to account for the vascular signal contribution. The application of either of the alternative (more complex) models enables the 'pseudopermeability' effect to be avoided and hence improves the patho-physiological specificity of the obtainable parameters. The excellent correlation between the two models of estimates of K^{trans} and v_p allow us to conclude that both models are valid for the evaluation of microvascular characteristics in tumours. This could enable monitoring of anti-angiogenic treatment effects and might also be valuable after radiation therapy for the differentiation of tumour recurrence and radiation induced necrosis. The shortness of time needed for acquisition of data when the first-pass model is applied is potentially useful, especially in studies outside the head, as it makes breath-hold image acquisition more feasible. In patients with low tolerability of the MRI environment this may also be a benefit in studies in the head.

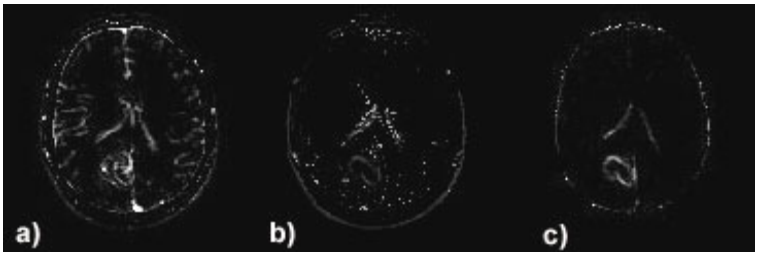

Figure 1. K^{trans} maps derived from the TK, mTK and FP model.

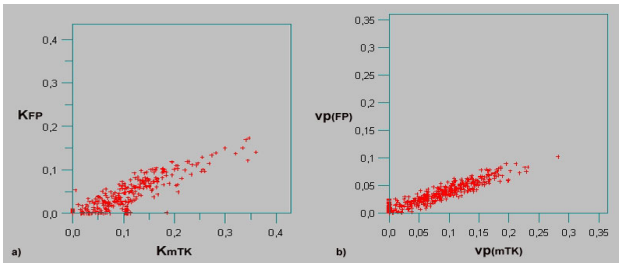

References

1. Parker, G.J.M. and Padhani, A.R., *in: Tofts P, ed. Quantitative MRI of the brain*, 342, 2003.
2. Padhani, A.R. and Husband, J.E., *Clin Radiol*,56, 607, 2001.
3. Tofts, P.S. and Kermode, A.G., *Magn Reson Med*, 17, 357, 1991.
4. Jackson, A., *et al., Brit J Radiol*, 76, 153, 2003.
5. Buckley, D.L., *Magn Reson Med*, 47, 601, 2002.
6. Parker G.J.M., *et al., 11th Meeting of the ISMRM* 2003, 1264
7. Daldrup H., E., *et al., Magn Reson Med*, 40, 537, 1998.
8. Li, K.L., *et al. J Magn Reson Imaging*, 12, 347, 2000.
9. Li, K.L. and Jackson, A., submitted to *J Magn Reson Imaging*

.

Acknowledgements

J.U.H. was supported by the German Society for Clinical Neurophysiology and Functional Imaging (DGKN).